

Selection of the optimal microelectrode during DBS surgery in Parkinson's patients

Konrad Ciecierski¹, Zbigniew W. Raś^{2,1}, and Andrzej W. Przybyszewski³

¹ Warsaw Univ. of Technology, Institute of Comp. Science, 00-655 Warsaw, Poland

² Univ. of North Carolina, Department of Comp. Science, Charlotte, NC 28223, USA

³ Univ. of Massachusetts Medical School, Dept. of Neurology, Worcester, MA 01655, USA

Abstract. Deep brain stimulation (DBS) of the subthalamic nucleus (STN) is effective treatment of Parkinson disease. Because the STN is small (9 X 7 X 4 mm) and it is not well visible using conventional imaging techniques, multi-microelectrode recordings are used to ensure accurate detection of the STN borders. Commonly used discriminations which microelectrode's signal relates to the activity of the STN are signal quality and neurologist's experience dependent. The purpose of this paper is to determine the STN coordinates in a more objective way. We present analysis of the neurological signals acquired during DBS surgeries. The purpose of our method is to discover which one of the scanning microelectrodes reaches the target area guaranteeing a most successful surgery. Signals acquired from microelectrodes are first filtered. Subsequently the spikes are detected and classified. After that, new signal is reconstructed from spikes. This signal's power is then calculated by means of FFT. Finally cumulative sum of the signal's power is used to choose a proper electrode.

The ultimate goal of our research is to build a decision support system for the DBS surgery. A successful strategy showing which of the recording microelectrodes should be replaced by the DBS electrode is probably the most difficult and challenging.

Keywords: Parkinson's Disease, DBS, STN, Wavelet, Filtering, PCA, FFT, Spike detection, Spike discrimination, Spike clustering

Introduction

The Parkinson's disease (PD) is a chronic, progressive movement disorder that affects the lives of at least one million patients across the United States and the number of PD patient is constantly increasing as effect of the population. The characteristic motor symptoms of PD, predominantly due to progressive degeneration of nigral dopaminergic neurons, are initially subtle and impact purposeful movement, and are often difficult to diagnose and to differentiate from other age related symptoms. Among it's symptoms there is an impairment of motor skills: tremor, stiffness and slowness of voluntary movements.

Subthalamic nucleus (STN) deep brain stimulation (DBS) has become the standard treatment for patients with advanced Parkinson's disease (PD) who have intolerable drug-induced side effects or motor complications after the long-term use of dopaminergic drugs. In this surgical procedure microelectrodes are inserted into brain on the track towards estimated from the MRI STN position. When they reach the destination, signal from them is being analyzed and upon the result of this analysis the trajectory of one of them is later used for implantation of the permanent DBS electrode. When the permanent electrode is activated, it disrupts abnormal activity of the STN and the impairment of motor skills to some degree lessens. To minimize the collateral damage to the brain tissue, it is imperative to use as few probing electrodes as possible, and to find the correct trajectory in most precise way.

1 Initial signal analysis

1.1 Removal of low frequency components

Recorded signal has to be initially processed before further analysis can begin. Often the signal is contaminated with low frequency components. This low frequencies comes both from biological and non-biological sources. One source in particular is worth mentioning - it's the frequency of power grid 50 Hz in Europe and 60 Hz in US. Below, a raw signal is shown (see Fig. 1) that was actually recorded within patients brain. In this recording one can clearly see that signal has strong component of low frequencies. This low frequencies affects the amplitude of the signal and the same it is very difficult to make any amplitude-based analysis. This is why signal needs be filtered. All frequencies below 375 Hz and above 3000 Hz were removed. and the resulting signal (see Fig. 2) is much more suited for further use.

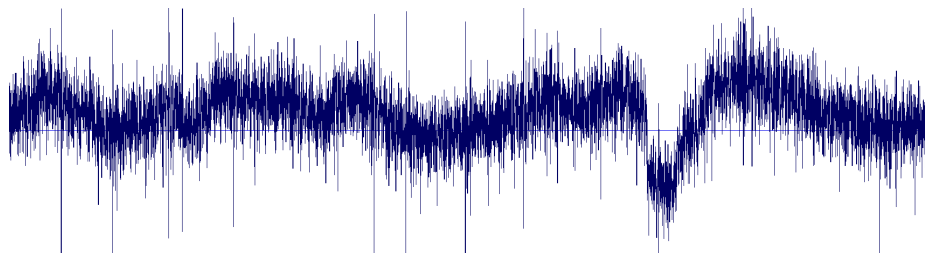


Fig. 1. Intraoperative 1s microelectrode recording from the sunthalamic area. The low frequency oscillations are clearly visible. One can also clearly see 10 spikes having amplitude much larger than the rest of the signal, but there are many other spikes with smaller amplitudes.

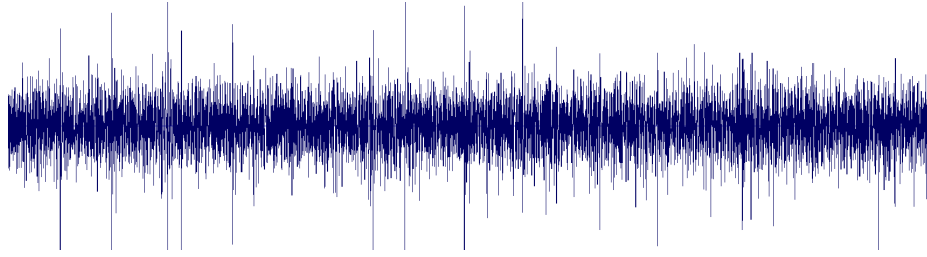


Fig. 2. The same 1s signal as in Fig. 1. but with frequencies below 375 Hz removed. One can still clearly see 10 spikes.

1.2 Spike shape retention

The process of high band filtering absolutely must retain the spikes that were observed in the raw signal. If only the presence of the spikes must be preserved, one can use FFT filtering. Using FFT is not suitable when not only occurrence but also the shape of the spikes should be preserved. This is because FFT strongly interferes with the shape of the spikes (see Fig. 3). This is why Daubechies D4 wavelet filtering was chosen as the filtering method. This idea of wavelet decomposition, filtering and reconstruction of DBS recorded signal has been described in [4]

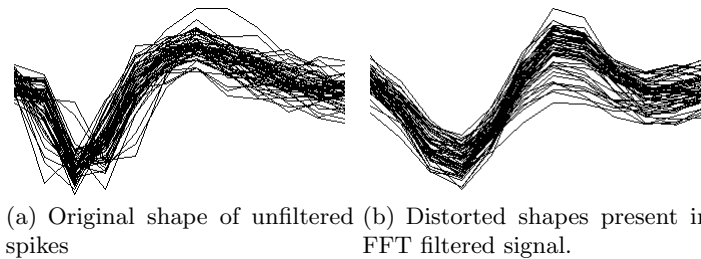


Fig. 3. Comparison of spike shapes in raw (a) and FFT filtered (b) signal.

2 Spike detection

As it was stated in [2], it is possible to detect spikes occurring in cells within radius of $50 \mu\text{m}$ from the electrode's recording tip. Still, this small area may contain around 100 neuronal cells. Recorded spikes from such area with one microelectrode may have different widths, shapes and amplitudes. Cells that are close to electrode will be recorded with a higher amplitudes then those being distal. Distance between electrode and soma can also have an influence on the

width of the recorded spike [3]. The greater the distance, the wider become recorded spikes from the same cell. All above makes the task of detecting spikes and discriminating them from the noise even more difficult. Two approaches to spike detection were considered:

2.1 Derivative approach

In this approach spikes detection bases on the slope of their amplitude. If the first derivative is below and then above some given thresholds during some consistent period of time then it is assumed that spike might have occurred. Assuming that amplitude over time is represented by $f(t)$, it's derivative as $f'(t)$, lower threshold as d_l and upper threshold as d_u . Necessary condition for spike to occur around time t_0 is shown on equation 1. Equations 2 and 3 guarantee that at some points the pitch of descent and ascent are greater then appropriate thresholds.

$$\exists t_b < t_0 < t_e (\forall (t_b < t < t_0) f'(t) < 0 \text{ and } \forall (t_0 \leq t < t_e) f'(t) \geq 0) \quad (1)$$

$$\exists (t_b < t_l < t_0) f'(t_l) < d_l \quad (2)$$

$$\exists (t_0 < t_u < t_e) f'(t_u) > d_u \quad (3)$$

It must also be mentioned that spikes with polarity negative to described above do exist and have to be detected in adequate, similar way.

2.2 Amplitude approach

Assuming that low frequency components have been already filtered out from the signal, one can attempt to detect spikes using amplitude analysis. In [5] it is postulated to use a specific amplitude threshold for spike detection. Threshold is there given by value V_{thr} (see equation 4) with $\alpha_{thr} \in \langle 4.0, 5.0 \rangle$. In this work different α_{thr} are begin used. During spike detection, program checks for spikes with values 5.0, 4.9, \dots , 4.0. Spike is assumed to exist when amplitude is lower then $-V_{thr}$ or higher then V_{thr} . If for some recording at given α_{thr} value, at least 200 spikes are found then it is accepted. If not, lower values are tested. If at value of 4.0 less then 30 spikes are found it is assumed that no representative spikes have been found. Advantage of this approach over the previous one is that in this case, the threshold can be calculated automatically. This allows the process of spike detection to be done in unsupervised - automatic way.

$$V_{thr} = \alpha_{thr} \sigma_n \quad \text{where} \quad \sigma_n = \frac{1}{0.6745} \text{median}(|x_1|, \dots, |x_n|) \quad (4)$$

2.3 Comparison of Approaches

Because of the ability of automatic spike detection, the amplitude approach was chosen. Regardless which approach i selected, some fine tuning is still necessary. This fine tuning is defined as zones of forbidden amplitude and is shown in red

(see Fig. 4). In case of *down – up* spikes (see Fig. 4(a)) the $-V_{thr}$ amplitude is shown as green line. Assuming that amplitude is below $-V_{thr}$ at time t_0 then spike occurs between $t_0 - 0.5 ms$ and $t_0 + 1.1 ms$ if fulfilled are conditions (5) \cdots (8). In case of *up – down* spikes (see Fig. 4(b)) the green line denotes V_{thr} amplitude level. Conditions (5) \cdots (8) must be modified in this case to reflect reversed amplitude.

$$\forall(t_0 - 0.5 ms < t < t_0 - 0.4 ms) \quad f(t) > -\frac{V_{thr}}{2} \quad (5)$$

$$\forall(t_0 + 0.4 ms < t < t_0 + 1.1 ms) \quad f(t) > -\frac{V_{thr}}{2} \quad (6)$$

$$\forall(t_0 - 0.5 ms < t < t_0 - 0.3 ms) \quad f(t) < \frac{V_{thr}}{2} \quad (7)$$

$$\forall(t_0 + 1.0 ms < t < t_0 + 1.1 ms) \quad f(t) < \frac{V_{thr}}{2} \quad (8)$$

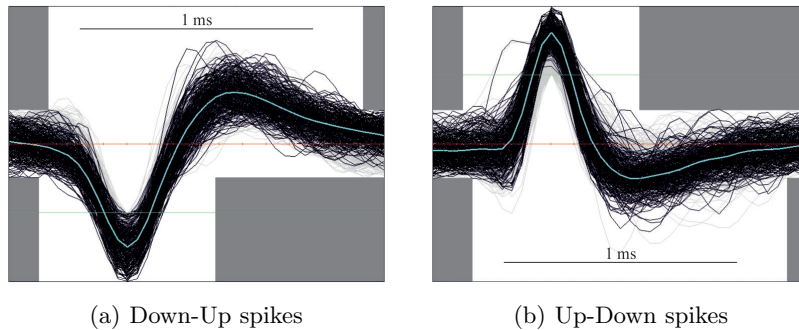


Fig. 4. Forbidden spike amplitude areas: in (a) 264 spikes, in (b) 266 spikes

3 Spike clustering

As mentioned in section 2, scanning electrode can register spikes coming from about 100 neurons. Not all of them are of the same cell type. Different neurons types/classes have different spike shapes. While it seems that shape alone is not sufficient to determine location of the electrode in patient's brain, it still unsubtly carries information that can be used in further analysis.

3.1 Clustering using PCA over spike amplitude

Archer et. al. in [5] use Principal Component Analysis to obtain principal component vectors and then use mean of the first few to obtain dominant spike shape. Here a modified PCA approach has been applied. Knowing that all spikes from given recording are 1.6 *ms* wide (see section 2.3) one knows that they are described using the same number of samples. It is so possible to build matrix containing all detected spikes with each row containing single spike. After the PCA is preformed the first ten most important principal component vectors are clustered using *k – means* method. Resulting cluster gives good spike shape discrimination.

3.2 Clustering using PCA over wavelet decomposition

To the shape of the spike, lower frequency components contributes the most. Comparing the wavelet transforms of different spikes also shows that the lower frequencies are most differentiating. Because of that, to enhance the effectiveness of the clustering, a subset of wavelet transform coefficients is used as the input to the PCA. Following approach used in [6], each spike is transformed using the *4levelHaar*, wavelet transform. Matrix containing row by row wavelet transformations of all spikes is then constructed. It is obvious that not all columns are needed for clustering. Some of them (esp. those related to higher frequencies) are redundand. Proper columns are chosen using modified Kolomogorov-Smirnov test (see [6]). The outcome of the PCA is used to obtain clusters in the same way as in (3.1)

3.3 Clustering summary

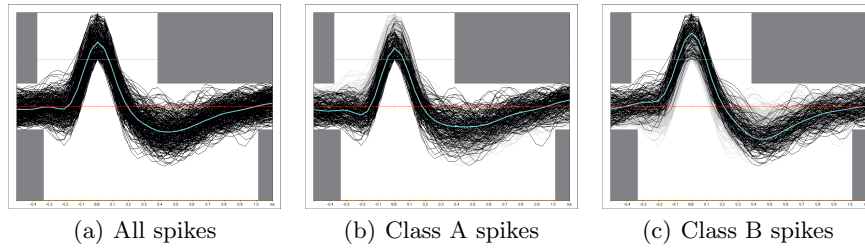
Both types of clustering produce good spike shape discrimination. In the (3.1) approach all spike data are being used as an input into PCA. This sometimes produces additional clusters. This clusters represent shapes that are similar to shapes yielded by other clusters and are different mainly in higher frequencies. Table 1 shows comparison of clustering results run on 96 recordings. For each clustering type it is shown how many recordings produced given number of different clusters/shapes. In both clustering approaches most recordings produced only 2 different shapes (73 recordings for amplitude based, and 62 recordings for wavelet based). Only in 9 and 15 respectfully recordings single shape class was detected. Fig. 5 shows example of spike discrimination. In processed recording 312 spikes were found (Fig. 5(a)). Spikes were subsequently divided into two shape classes containing 167 (Fig. 5(b)) and 125 (Fig. 5(c)) spikes.

4 Power spectrum analysis

The area of the brain in which electrode should be inserted (*STN*) is characterized by high neuronal activity. This activity should be reflected in power of the

Table 1. Cluster size occurrence

<i>Shapes detected</i>	<i>Amplitude based</i>	<i>Wavelet based</i>
1	9	15
2	73	62
3	11	17
4	2	2
5	1	0

**Fig. 5.** An example of the spike discrimination: a) 312 spikes, b) 167 spikes, c) 125 spikes.

signal. The raw recorded signal is highly contaminated with noise from neurons that are near the electrode. In [7], authors basing upon spikes occurrence in original signal create new one to conduct the synchronization analysis. In this paper similar procedure is used to create the temporary signal from the spikes and then analyze it's power using FFT.

4.1 Creating the temporary signal

The temporary signal has the same length as the original one. Its sample rate is 1 KHz. This sample rate according to Nyquist-Shannon sampling law ensures that frequencies up to 500Hz will be well described. Signal is created with constant amplitude 0, then at points that correspond to spike occurrences, a part of cosine function is inserted. Cosine function values are inserted in such a way that if the spike occurred at time t_0 then a part of cosine defined on $\langle -\frac{\pi}{2}, \frac{\pi}{2} \rangle$ is mapped onto $\langle t_0 - 5ms, t_0 + 5ms \rangle$. Mapping is done in additive way - if two or more spike induced cosines overlap they amplitudes summarize.

4.2 Extracting the power spectrum

When all spikes have their representation in the temporary signal, it is transformed using FFT to obtain the power spectrum. It is possible to obtain power spectrum for frequencies up to 500Hz. Power of the frequencies above 100Hz is very small and as frequency increases it quickly approaches zero. Because of that,

only for frequencies less or equal 100Hz power spectrum is being observed, power of higher frequencies is discarded. Power for frequencies below 1Hz is also not taken into account, it comes from all spikes being separated from each other by 1s or more and not STN specific. Summarizing, power is calculated for frequency range from 1Hz to 100Hz with resolution 1Hz.

4.3 Power analysis

In DBS surgery several electrodes traverse selected hemisphere on parallel trajectories towards the STN. Electrodes record potentials at the same time and for the same time period. It is safe to compare the power of the signal recorded in these electrodes. Assume that for a given electrode e the power of a signal recorded at depth d , calculated for frequency f is represented by $pwr(e, d, f)$. This cumulative power can be defined as shown by equation (9)

$$pwr_{cumul}(electrode, depth) = \sum_{d \leq depth} \sum_{f=1}^{100} pwr(electrode, d, f) \quad (9)$$

4.4 Usefulness of cumulative power

Cumulative power have some interesting properties that can be useful to neurosurgeons and neurologists.

Test data. The dataset contain recordings taken from 11 DBS surgeries. During surgeries there were 20 sets of the microelectrode recordings. Each set contained from 2 up to 4 microelectrodes; total 60 probing microelectrodes were used. In all sets, neurologists have selected one of the electrodes as trajectory for implantation of final, stimulating electrode.

Selecting electrode that will reach the STN with good accuracy. When the microelectrodes reach the estimated from MRI depth at which STN should be found, it is time to pick one of them as a trajectory for the final stimulating electrode. If at this final depth, a cumulative power is calculated for each of the scanning electrodes, then obtained values can be used to determine position of the DBS electrodes. Microelectrodes with higher value of cumulative power are far more likely to be the ones that actually have reached the STN. The cumulative power has been calculated for all (60) microelectrodes from our dataset. If highest cumulative power was used as the criterium for selecting electrode from a given probing set, then 13 out of 20 good electrodes would be correctly selected. Specificity is 0.85, sensitivity is 0.62. See Table 2(a). In four sets, the electrode chosen by neurologist has 2nd highest cumulative value. If highest or 2nd highest cumulative power were used as criterium for selecting electrodes from a given probing set, then 17 out of 20 good electrodes would be correctly selected. Specificity is 0.85, sensitivity is 0.71. See Table 2(b).

(a)				(b)			
	positive	negative	%		positive	negative	%
true	13	33	76.7%	true	17	33	83.3%
false	6	8	23.3%	false	6	4	16.7%

Table 2. Classification results

Predicting if electrodes are likely to reach the STN or not. It is desirable to know, as quickly as possible, if a given microelectrode is going to reach the STN or not. If we know that a given microelectrode has minimal chance to reach the target, a neurosurgeon would not have to advance it deeper in the brain decreasing this way chances for additional side effects. Fig. 6 shows that already at the depth -1000 (1mm above estimated target position) one may suspect that *Anterior* microelectrode might be the best one (highest steepness) and that *Lateral* microelectrode will most probably miss the target.

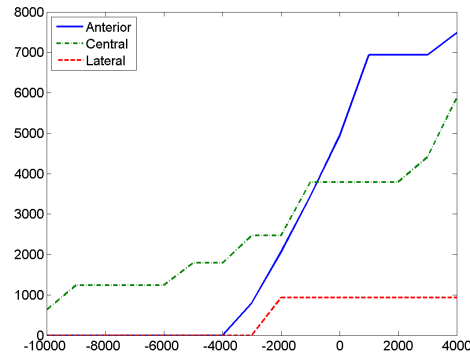


Fig. 6. Changes in cumulative power of signals simultaneously recorded from three microelectrodes over the depth

Pinpointing depth of the microelectrode which reached the STN. In some cases only one probing electrode is inserted into patient's brain. It is then impossible to compare it with other data. Still the cumulative power gives us some information regarding whether and when electrode reached the STN. Fig. 7 shows that from depth of -5, the power of the signal steeply increases. With high probability this is the depth about which STN has been reached.

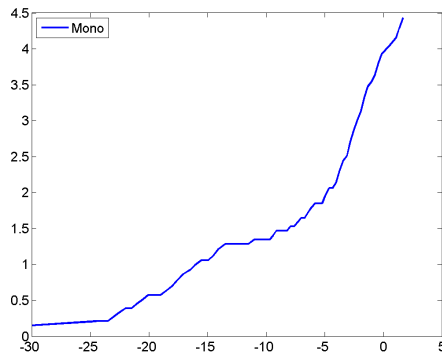


Fig. 7. Changes in cumulative power signal recorded from single microelectrode over the depth

5 Conclusions

We propose that the spike shape extraction, classification and their cumulative power spectra are new tools that might help to determine the exact STN coordinates. Our decision algorithm will increase surgery safety and improve precision of the STN stimulation that will make the DBS therapy more efficient.

References

1. Darrell A. Henze, Zsolt Borhegyi, Jozsef Csicsvari, Akira Mamiya, Kenneth D. Harris, Gyrgy Buzski. Intracellular Features Predicted by Extracellular Recordings in the Hippocampus In Vivo *Journal of Neurophysiology* 2000 84:390-400
2. Klas H. Pettersen, Gaute T. Einevoll. Amplitude Variability and Extracellular Low-Pass Filtering of Neuronal Spikes *Biophysical Journal*, 2008 94: 784-802
3. Claude Bédard, Helmut Krüger and Alain Destexhe. Modeling Extracellular Field Potentials and the Frequency-Filtering Properties of Extracellular Space *Biophysical Journal*, 2004 86: 1829-1842
4. Alexander B. Wiltschko, Gregory J. Gage, and Joshua D. Berke. Wavelet Filtering before Spike Detection Preserves Waveform Shape and Enhances Single-Unit Discrimination *J Neurosci Methods*. 2008, 173: 34-40
5. Archer, C. and Hochstenbach, M.E. and Hoede, C. and Meinsma, G. and Meijer, H.G.E. and Ali Salah, A. and Stolk, C.C. and Swist, T. and Zyprych, J Neural spike sorting with spatio-temporal features *Proceedings of the 63rd European Study Group Mathematics with Industry*, 28 Jan - 1 Feb 2008
6. Quiñan Quiroga, R. and Nadasdy, Z. and Ben-Shaul, Y. Unsupervised Spike Detection and Sorting with Wavelets and Superparamagnetic Clustering MIT Press 2004
7. Ron Levy, William D. Hutchison, Andres M. Lozano, and Jonathan O. Dostrovsky High-frequency Synchronization of Neuronal Activity in the Subthalamic Nucleus of Parkinsonian Patients with Limb Tremor *The Journal of Neuroscience*, 2000, 20:7766-7775